XIX International Conference on Water Resources
CMWR 2012
University of Illinois at Urbana-Champaign
June 17-22,2012

COMPUTATIONALLY EFFICIENT NUMERICAL MODEL FOR THE EVOLUTION OF DIRECTIONAL OCEAN SURFACE WAVES

Matt Malej*, Arnaud B. Goullet† and Wooyoung Choi†

* Coastal and Hydraulics Laboratory
U.S. Army Engineer Research and Development Center
3909 Halls Ferry Road, Vicksburg, MS 39180 USA
e-mail: matt.malej@usace.army.mil

† New Jersey Institute of Technology
Department of Mathematical Sciences
Center for Applied Mathematics and Statistics
University Heights, Newark, NJ 07102

Key words: rogue waves, spectral methods, asymptotic models, Dirichlet-to-Neumann operator

Summary. This paper concerns a development of a new efficient numerical model for the short term prediction of evolving weakly nonlinear ocean surface waves. By extending the works of West *et al.* [1] and Choi[2], and utilizing the fact that waves in the ocean tend to travel primarily in one direction, this new numerical model is derived based on additional assumption of a weak transverse dependence. The model is implemented via Fourier pseudo-spectral method and numerous Monte-Carlo random numerical simulations are carried out. The new model is shown to behave quite well in various directional wave fields and can potentially be a candidate for the prediction and propagation of large ocean surface waves known as Rogue or Freak waves.

1 INTRODUCTION

Large amplitude ocean waves whose height surpasses twice the significant wave height of the analyzed field, commonly referred to as Rogue or Freak Waves, have been known to occur more frequently by improvements in remote sensing technology than what people would have expected. Consequently, a considerable effort has been made towards a better understanding of the occurrence of highly nonlinear ocean waves over the course of the last decade. Several physical mechanisms have been suggested as plausible agents behind the generation and extended propagation of these extreme waves. These can include, focusing due to modulational instability, wave-current interaction, atmospheric forcing, soliton collisions, as well as geometrical (spatial) and dispersive (spatio-temporal) focusing. Though the modulational instability, also referred to as Bejnamin-Feir instability, is usually exhibited in the propagation of long-crested waves, its presence in the creation of extreme waves in the form of resonant and quasi-resonant interactions is becoming more evident[3,4]. This is

essentially a nonlinear phenomenon of uniform wavetrains with unstable sidebands, which produces growing amplitude modulations. These modulations, in turn, evolve into groups of steep waves due to nonlinear focusing of wave energy. Subsequently, at the very maximum of the modulation, extreme (Rogue) waves can emerge, followed by the demodulation and often recurrence to a nearly uniform wavetrain.

In terms of waves with broad directional distribution, it has been shown by that as directional distribution broadens, the occurrence of these uncommonly large waves subsides[5,6]. These findings were normally supported via statistical methods, such as a measure of the fourth statistical moment (kurtosis)[7,8]. In contrast, Waseda and collaborators have analyzed operational data from the northern regions of the North Sea and showed that a valid precursor for the onset of these large waves is a spectrum with a narrow angular distribution[9].

Computing efficiently and accurately the evolution of highly nonlinear time-dependent, three-dimensional surface wave fields in various ocean environments is certainly a challenging hydrodynamic problem. While it is believed that these extreme waves are more than the mere random superposition of different wave components, a common assumption in modeling ocean waves is that the sea state is a stationary random process. This tends to give a false impression on the frequency of the occurrence of these extremely large waves. Most models commonly used for describing such phenomenon are far from being complete and rely on ad-hoc models for physical processes involved. For a more accurate model, a large number of factors need to be considered such as: variable bottom topography, ocean currents, wave-wind interactions and energy dissipation due to wave breaking. An additional complication is that there is a wide range of scales to be resolved. The coupling between various modes and thus the energy transfer between different length scales lack a thorough understanding. Even these models, often written in terms of wave spectrum, are still highly complex and do not possess analytic solutions and hence require careful and costly numerical computations.

2 MATHEMATICAL FORMULATION

2.1 Governing equations for water waves

Under the assumption of an inviscid and irrotational flow, the velocity vector can be expressed as the gradient of a scalar potential $\mathbf{u} = \nabla_3 \phi$, where ∇_3 is the three-dimensional gradient. For an incompressible fluid, the governing equation in the main fluid body for the velocity potential is the three-dimensional Laplace equation

$$\nabla^2\phi + \frac{\partial^2\phi}{\partial z^2} = 0 \qquad\qquad -h \leq z \leq \zeta(\bar{x}, t), \tag{1}$$

where ∇ is the horizontal gradient defined as $\nabla \equiv (\partial/\partial x, \partial/\partial y)$. Assuming no variable bottom topography, the bottom boundary condition at $z = -h$ is the no-flux condition in the form of

$$\frac{\partial\phi}{\partial z} = 0. \tag{2}$$

At the free surface ($z = \zeta(x, y, t)$) the kinematic and dynamic boundary conditions are given, respectively, by

$$\frac{\partial\zeta}{\partial t} + \nabla\phi \cdot \nabla\zeta = \frac{\partial\phi}{\partial z}, \tag{3}$$

$$\frac{\partial \phi}{\partial t} + \frac{1}{2}|\nabla \phi|^2 + \frac{1}{2}\left(\frac{\partial \phi}{\partial z}\right)^2 + g\zeta = 0, \tag{4}$$

where g is the acceleration due to gravity. It should perhaps be also pointed out that, since in this study we are mainly concerned with the gravity waves, we neglect the effects of surface tension, whose significance would be substantiated if the characteristic wavelengths were $O(1\ cm)$.

2.2 Small wave steepness asymptotics for fully two-dimensional waves

The fully two-dimensional model is based on the work of West and collaborators[1]. The general idea is to obtain an asymptotically reduced system, based on a small wave steepness assumption ($\epsilon \ll 1$), for the surface elevation ζ and the velocity potential evaluated at the free-surface [$\Phi = \phi(\bar{x}, z = \zeta, t)$]. When the free surface boundary conditions (3)-(4) are written in terms of the two canonical variable ζ and Φ, we obtain

$$\frac{\partial \zeta}{\partial t} + \nabla\Phi \cdot \nabla\zeta = \left(1 + |\nabla\zeta|^2\right) W, \qquad \frac{\partial \Phi}{\partial t} + \frac{1}{2}|\nabla\Phi|^2 + g\zeta = \frac{1}{2}\left(1 + |\nabla\zeta|^2\right) W^2, \tag{5}$$

where $W \equiv \frac{\partial \phi}{\partial z}(\bar{x}, z = \zeta, t)$. In doing so, one is faced with a need of defining a non-local integral operator that gives the constituent relation between the velocity potential Φ at the free-surface and its vertical velocity W. The result yields the fully two-dimensional (F2D) model accurate to third order in wave steepness in the following dimensional form

$$\frac{\partial \zeta}{\partial t} + \mathcal{L}[\Phi] + \nabla(\zeta\nabla\Phi) + \mathcal{L}[\zeta\mathcal{L}[\Phi]] + \nabla^2\left(\frac{\zeta^2}{2}\mathcal{L}[\Phi]\right) + \mathcal{L}\left[\frac{\zeta^2}{2}\nabla^2\Phi + \zeta\mathcal{L}[\zeta\mathcal{L}[\Phi]]\right] + O(\epsilon^4) = 0, \tag{6}$$

$$\frac{\partial \Phi}{\partial t} + g\zeta + \frac{1}{2}|\nabla\Phi|^2 - \frac{1}{2}\left(\mathcal{L}[\Phi]\right)^2 - \mathcal{L}[\Phi]\left(\zeta\nabla^2\Phi + \mathcal{L}[\zeta\mathcal{L}[\Phi]]\right) + O(\epsilon^4) = 0, \tag{7}$$

where ϵ is the wave steepness. The nonlocal operator $\mathcal{L}$, commonly referred to as a Dirichlet-to-Neumann operator, is defined in Fourier ($\mathcal{F}$) space as $\mathcal{F}\left[\,\mathcal{L}[\Phi]\,\right] = -\kappa\,\tanh(\kappa h)\hat{\Phi}$, with $\kappa = \sqrt{k_x^2 + k_y^2}$ and $\hat{\Phi} = \mathcal{F}[\Phi]$, where k_x and k_y are the wave numbers in the x and y directions, respectively.

2.3 Weakly two-dimensional model

Since ocean waves tend to travel primarily in one direction (say the x-direction), our weakly two-dimensional (W2D) model is based on additional assumption of weak transverse dependence. In that respect, the weak transverse assumption is exhibited through the wavenumber ratio k_y/k_x being small, so that $\kappa\tanh(\kappa h) = \sqrt{k_x^2 + k_y^2}\,\tanh\left(\sqrt{k_x^2 + k_y^2}\,h\right)$ can be expanded to a desired order. How small the ratio should be is a matter of predefined initial velocity wave field and we set the ratio k_y/k_x to be $O(\epsilon)$, where ϵ is defined to be the product of characteristic wave amplitude and peak wavenumber ($\bar{a}\,k_p$). By collecting terms of the third order in wave steepness ϵ, the modeled equations for arbitrary water depth are

given, in their symbolic Fourier form, by

$$\begin{aligned}\zeta_t + |k_x|\left(1+\tfrac{1}{2}\left(\tfrac{k_y}{k_x}\right)^2\right)\tanh(|k_x|h)\Phi + |k_x|\left(\tfrac{|k_x|h}{2}\left(\tfrac{k_y}{k_x}\right)^2\operatorname{sech}^2(|k_x|h)\right)\Phi + (ik_x\zeta\, ik_x\Phi - \zeta k_x^2\Phi)\\ +|k_x|\tanh(|k_x|h)\left(\zeta|k_x|\tanh(|k_x|h)\Phi\right) - k_x^2\left(\tfrac{\zeta^2}{2}|k_x|\tanh(|k_x|h)\Phi\right)\\ +|k_x|\tanh(|k_x|h)\left(-\tfrac{\zeta^2}{2}k_x^2\Phi + \zeta|k_x|\tanh(|k_x|h)(\zeta|k_x|\tanh(|k_x|h)\Phi\right) + O(\epsilon^4) \;=\; 0,\end{aligned} \tag{8}$$

$$\begin{aligned}\Phi_t + g\zeta + \tfrac{1}{2}(ik_x\Phi)^2 - \tfrac{1}{2}(|k_x|\tanh(|k_x|h)\Phi)^2\\ -|k_x|\tanh(|k_x|h)\Phi\left(-\zeta k_x^2\Phi + |k_x|\tanh(|k_x|h)\left[\zeta|k_x|\tanh(|k_x|h)\Phi\right]\right) + O(\epsilon^4) \;=\; 0.\end{aligned} \tag{9}$$

The above mentioned symbolic Fourier form can be viewed, for example, as

$$k_x^2\left(\frac{\zeta^2}{2}|k_x|\tanh(|k_x|h)\Phi\right) \;\equiv\; \mathcal{F}^{-1}\left[k_x^2\,\mathcal{F}\left[\frac{\zeta^2}{2}\,\mathcal{F}^{-1}\{|k_x|\tanh(|k_x|h)\mathcal{F}[\Phi]\}\right]\right],$$

where $\mathcal{F}$ and $\mathcal{F}^{-1}$ are the forward and backward Fourier transforms, respectively. What should be immediately apparent in equations (8) and (9) is that we have only two terms with transverse dependence (k_y). That very same point has advantages for numerical computation and is furthered discussed in the subsequent sections.

3 NUMERICAL SIMULATIONS

3.1 Numerical method and initialization

To solve numerically the F2D and W2D models, we adopt a Fourier pseudo-spectral method, similar to that of Lo and Mei[10], with the periodic boundary conditions, where the surface elevation (ζ) and the velocity potential (Φ) are expressed as a superposition of individual Fourier modes. We integrate the system via a fourth-order Runge-Kutta method with a set time step of $\Delta t/T_p = 10^{-3}$, which conserves all of the physical conserved quantities including mass, momentum, and energy to a very high degree of accuracy. Notice that, for the third-order model, we apply a low pass filter to set to zero a half of Fourier modes at every time step to avoid aliasing errors.

In order to describe a realistic ocean wave field, we designate the Fourier transform of the auto-correlation function $F(\mathbf{k}) = F(k,\theta) = S(k)\,D(\theta)$ of surface elevations as our initial spectrum, where k and θ are the polar coordinates of (k_x, k_y), and for $S(k)$ we utilize the JONSWAP spectrum

$$S(k) = \frac{\alpha\, k_p^2\, H_s^2}{2\,k^4}\exp\left(-\frac{5}{4}\left(\frac{k_p}{k}\right)^2\right)\gamma^{\exp\left(-(\sqrt{k/k_p}-1)^2/(2\sigma_A^2)\right)}. \tag{10}$$

The peak wavenumber k_p is obtained through linear dispersion relation $\omega_p^2 = gk_p\tanh(k_ph)$, the coefficient γ is known as the peak enhancement, while the parameter $\sigma_A = (0.07, 0.09)$ for $(k > k_p, k < k_p)$. In addition, the dimensional parameter α, known as the Phillips parameter, was taken to be $5/16$. By the same token, based on the relatively narrow spectral bandwidth, we can define the wave steepness as the product of twice the standard deviation

and the peak wavenumber ($\epsilon = 2k_p\sigma$), where $\sigma = \left(\iint k\, F(k,\theta)\, dk\, d\theta\right)^{\frac{1}{2}}$. For the directional distribution function $D(\theta)$ the following form was used

$$D(\theta) = \begin{cases} \frac{1}{\beta}\cos^2\left(\frac{\pi\theta}{2\beta}\right) & \text{if} \quad |\theta| \leq \beta \\ 0 & \text{if} \quad |\theta| > \beta. \end{cases} \tag{11}$$

The initialization of the free-surface velocity potential is obtained from the linear theory. The value of the standard deviation σ is appropriately chosen through the input parameters so the wave steepness (ϵ) has a desired value and in the case of numerical simulation discussed next, its values are $\epsilon = 0.03, 0.05, 0.08$, and 0.13 (see Table 1). The initial spatial grid was comprised of $(N_x, N_y) = (512, 256)$ Fourier modes. We employed about 30 characteristic wavelengths ($\lambda_p = 2\pi/k_p \sim 1.5\,\mathrm{m}$) in each horizontal direction, with characteristic wave period of 1 sec. Though in realistic ocean wave fields the characteristic wave period is between 6 to 16 seconds, we can certainly (without a loss of generality) scale the system to accommodate our chosen characteristic wave period. Also, note that the case of $\epsilon = 0.1$ is, in fact, a rather extreme end of the spectrum, as it is illustrated by the scatter diagram of Statoil recordings in the work of Socquet-Juglard and his collaborators[6].

β	γ	k_p	$\lambda_p = \frac{2\pi}{k_p}$	T_p	H_s	$\epsilon = k_p\bar{a}$	$Time$	$\#\ of\ Runs$
0.14	5.0	4.02	1.56	1	0.0114	0.03	150	100
0.35	5.0	4.02	1.56	1	0.0180	0.05	150	200
0.7	3.3	4.02	1.56	1	0.0326	0.08	150	200
0.7	3.3	4.02	1.56	1	0.0515	0.13	150 & 900	100 & 100

Table 1: JONSWAP spectrum — Initial input and numerical simulation parameters. Here, β is the initial directional distribution parameter, γ is the peak enhancement, k_p is the peak wavenumber, λ_p is the peak wavelength (measured in meters). T_p is the characteristic (peak) wave period in seconds, ϵ is the wave steepness, $\bar{a}$ is the characteristic wave amplitude measured in meters, and $Time$ represents the physical duration of the simulations (in seconds). The $'\#\ of\ Runs'$ gives the total number of ensemble averaged random Monte-Carlo simulations for the given set of parameters.

From our daily experiences we know that the ocean waves behave irregularly and somewhat unpredictably on various time scales. Hence, the dynamics of ocean waves often manifest a random (stochastic) nature. In that respect, the sea surface at a given place and time can be represented by a random indexed function with some statistical properties. This approach is referred to as stochastic and aims at a statistical description of the sea surface. In the absence of open ocean wave field data, the goal would be to describe and predict the dynamics of certain realizations on the basis of ensemble averages. This approach, in fact, is widely used in ocean engineering and atmospheric research.

In order to obtain time dependent statistical properties, we can elect to perform stochastic (Monte-Carlo) simulations – that is, we can use our deterministic models to compute a sufficient number of randomly chosen realizations of the sea state. The premise behind it is that, if we take a sufficiently large number of random representations of the sea surface, then the ensemble average of this large (but finite) number of simulations would adequately represent the evolution of the whole ensemble (in statistical sense).

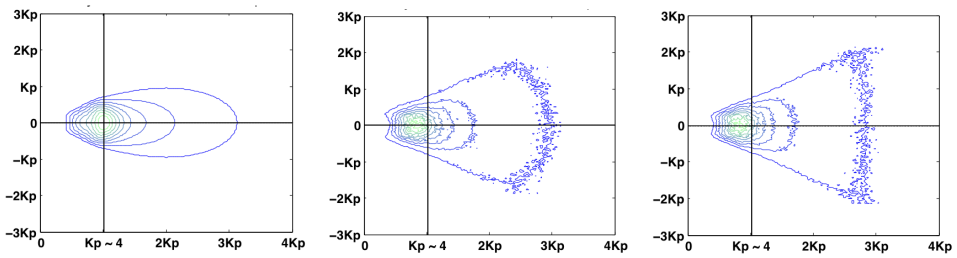

(a) Initial Condition (b) Fully 2D (c) Weakly 2D

Figure 1: **Case 3** – Evolution of the spectrum of initial directional distribution $\beta = 0.7$ (widest case) and wave steepness of $\epsilon = 0.08$. Figure (a) gives the initial density contour plot, while (b) and (c) represent the Fully 2D and Weakly 2D models, respectively, at 150 peak periods (150 sec), all averaged over 100 simulations. The black crossing lines mark the spot of the initial spectral peak (Kp).

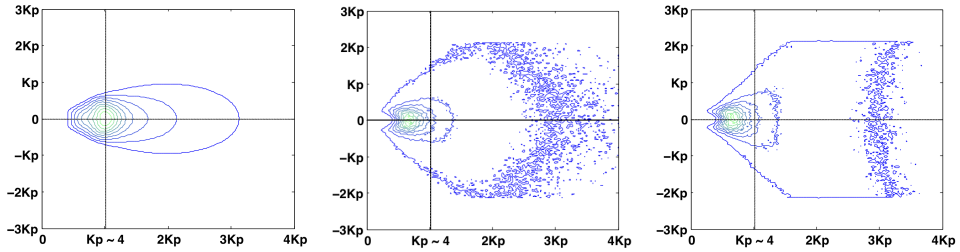

(a) Initial Condition (b) Fully 2D (c) Weakly 2D

Figure 2: **Case 4** – Evolution of the spectrum of initial directional distribution $\beta = 0.7$ and wave steepness of $\epsilon = 0.13$.

4 NUMERICAL RESULTS

In this section we compare the evolution of the spectra in the context of ensemble averages between the Fully 2D (F2D) and Weakly 2D (W2D) models. In addition, due to spatial discretization of initially smooth JONSWAP spectrum, the spectrum quickly loses its original smoothness. The averaging over 100 simulations allows us, in turn, to smooth out the spectrum in order to be able to clearly distinguish the level curves in the spectral density plots.

Since the W2D model is derived with an additional assumption of weak transverse dependence, it is expected that the two numerical solutions for relatively narrow initial directional distribution of $\beta = 0.14, 0.35$ and $\epsilon = 0.03, 0.05$ would yield good comparisons, and would show little spectral evolution as these would represent primarily weakly nonlinear cases. Hence, we elect to concentrate on the latter two cases $\beta = 0.7$ for $\epsilon = 0.08, 0.13$, that show appreciable spectral differences.

In Figure 1 the spectra at $t = 0$ and at $t/T_p = 150$ for the third case of directional distribution (11) with $\beta = 0.7$ and wave steepness of $\epsilon = 0.08$ is shown. In this case, the downshifting of the spectral peak which is commonly attributed to modulational (Benjamin-Feir) instability, marked by the intersecting two black marker lines, is quite evident. Though it should be noted that as our initial directional distribution is broadened, the nonlinearity (ϵ) is also being increased. Also, the tail of the spectrum between Weakly 2D and Fully 2D models is qualitatively different. This is also the case of for $\beta = 0.7$ and $\epsilon = 0.13$ (see Figure 2). We ultimately believe that this difference in the qualitative nature of the spectral tail is brought about the

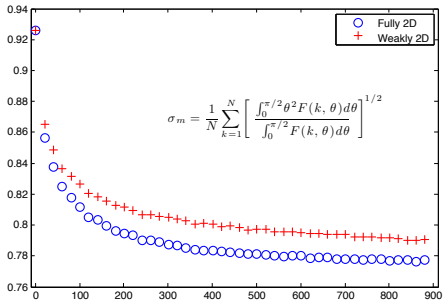

Figure 3: Mean Spreading Function of (12) plotted as a function of time for the final time of 900 seconds (900 peak periods). The wave steepness $\epsilon = 0.13$ and the initial directional spreading $\beta = 0.7$.

asymptotic limitations of the Weakly 2D model. Mainly, in the areas (corners) where the Weakly 2D spectrum (at $t/T_p = 150$) does not have the same curvature as the Fully 2D model, the ratio k_y/k_x, originally assumed to be of order of the wave steepness (ϵ), is no longer small.

To quantify in more detail the differences in spectral evolution of the Fully and Weakly 2D models we define the mean directional spreading function

$$\sigma_m(k) = \left(\frac{\int_0^{\pi/2} \theta^2 F(k,\theta)\mathrm{d}\theta}{\int_0^{\pi/2} F(k,\theta)\mathrm{d}\theta} \right)^{1/2}, \tag{12}$$

where hereafter $\sigma_m(k)$ will be averaged over the wavenumber k and referred to as σ_m. The results between the two models for $\beta = 0.14, 0.35$ are qualitatively identical, thus we again concentrate on the most nonlinear case $\beta = 0.7$, $\epsilon = 0.13$. In Figure 3 we show the mean spreading function for 100 averaged simulations up to 900 peak periods, where we can clearly observe a converging trend suggesting a quasi-steady-state for the mean spectral spreading function.

5 CONCLUSIONS

The focus of this paper has been the the development of an accurate phase-resolving numerical model for the short-term evolution of weakly nonlinear ocean surface waves. In that respect, our Weakly 2D model, based on additional assumption of weak transverse dependence, behaved qualitatively well in broad directional wave fields. One of the main advocates for the Weakly 2D model is its gain in the computational speed. Mainly, in Weakly 2D system (8)-(9) there are only two terms with the transverse wavenumber k_y. Hence, we can reduce the computation burden of the remaining terms by a half. In other words, wherever we have any x-derivative, which would correspond to k_x Fourier multiplier, we can elect to carry out only a 1D Fourier transform along the x-direction for every single y-component, thus essentially performing 50% of the operations required by a standard 2D FFT.

In summary, in the face of limited computational resources there is always a pressing need to reduce the cost of evaluation of hydrodynamic models without losing the level of necessary accuracy and preserving the desired coherent structures. The derivation of the Weakly 2D model was carried out with exactly that in mind. In fact, with the application to for instance naval hydrodynamics, this problem becomes even more acute in the context of ensemble modeling, which itself requires repeated forward and backward integrations of the model. In large

scale computational settings, reduced models capable of generating compact system representations that capture essential features of the fully articulated model with only a small loss of fidelity, offer enormous potential benefits to the operational utility of computational models.

ACKNOWLEDGEMENT

The authors gratefully acknowledge support from the U.S. Office of Naval Research through Grant No. N00014-05-1-0537 and the WCU (World Class University) program through the National Research Foundation of Korea funded by the Ministry of Education, Science and Technology (Grant No. R31-2008-000- 10045-0).

Permission was granted by the Chief of Engineers to publish this information.

REFERENCES

[1] B. J. West, K. A. Brueckner, R. S. Janda, M. Milder, and R. L. Milton. A new numerical method for surface hydrodynamics. *J. Geophys. Res.*, **92**, 11808–11824, (1987).

[2] W. Choi. Nonlinear evolution equations for two-dimensional surface waves in fluid of finite depth. *J. Fluid Mech.*, **295**, 381–394, (1995).

[3] T. Waseda, T. Kinoshita, and H. Tamura. Evolution of a random directional wave and freak wave occurrence. *J. Phys. Oceanogr.*, **39**, 621–639, (2009a).

[4] T. Waseda, T. Kinoshita, and H. Tamura. Notes and correspondences: interplay of resonant and quasi-resonant interaction of the directional ocean waves. *J. Phys. Oceanogr.*, **39**, 2351–2362, (2009b).

[5] M. Onorato, A. R. Osborne, and M. Serio. Extreme wave events in directional, random oceanic sea states. *Phys. Fluids*, **14**, 25–28, (2002).

[6] H. Socquet-Juglard, K. Dysthe, K. Trulsen, H. E. Krogstad, and J. Liu. Probability distributions of surface gravity waves during spectral changes. *J. Fluid Mech.*, **542**, 195–216, (2005).

[7] K. B. Dysthe. Note on a modification to the nonlinear Schrödinger equation for application to deep water waves. *Proc. R. Soc. Lond. A*, **369**, 105–114, (1979).

[8] A. Toffoli, O. Gradstad, K. Trulsen, J. Monbaliu, E. Bitner-Gregersen, and M. Onorator. Evolution of weakly nonlinear random directional waves: laboratory experiments and numerical simulations. *J. Fluid Mech.*, **664**, 313–336, (2010).

[9] T. Waseda, M. Hallestrig, K. Ozaki, and H. Tomita. Enhanced freak wave occurrence with narrow directional spectrum in the North Sea. *Geophys. Res. Lett.* **38**, L13605, (2011).

[10] E. Y. Lo and C. C. Mei. Slow Evolution of nonlinear deep-water waves in two horizontal directions: a numerical study. *Wave Motion*, **9**, 245–259, (1987).